Eur. Phys. J A 2, 41–53 (1998)

THE EUROPEAN PHYSICAL JOURNAL A

Probing the structure of exotic nuclei by transfer reactions

H. Lenske[1], G. Schrieder[2]

[1] Institut für Theoretische Physik, Universität Giessen D-35392 Giessen, Germany
[2] Institut für Kernphysik, TU Darmstadt D–64289 Darmstadt, Germany

Received: 1 October 1997 / Revised version: 25 November 1997
Communicated by D. Schwalm

Abstract. Low energy single nucleon transfer reactions are proposed as a tool to investigate the structure of nuclei far off stability. Experimental concepts and conditions are discussed, in particular high resolution γ-ray spectroscopy after single nucleon pickup reactions. Nuclear structure is described by Skyrme Hartree-Fock calculations including pairing. As representative examples, binding energies, radii and wave functions for Mg and Sn isotopes are calculated. In the neutron deficient Mg isotopes a proton skin is found. At the neutron driplines the Mg and Sn isotopes develop extended neutron skins. The nuclear structure results are used in DWBA and EFR-DWBA transfer calculations. Single nucleon transfer reactions of ^{32,36}Mg and exotic Sn beams on targets ranging from ^{2}H to ^{24}Mg in inverse kinematics are explored. The one-nucleon transfer cross sections decrease strongly for high-Z targets. An impact parameter analysis shows that the transfer process is selective on the tails of the wave functions. The largest cross sections are obtained for ^{2}H and ^{9}Be targets at incident energies of E_{lab} =2-5 MeV/u. The energy-momentum dependence is closely related to the special properties of wave functions of weakly bound states. Two-neutron (p,t) stripping reactions are studied for a ^{6}He projectile. A strong competition of sequential and direct processes is found at low energies.

PACS. 25.60.Je Transfer reactions – 21.60.Jz Hartree-Fock and random-phase approximations – 21.10.Gv Mass and neutron distributions

1 Introduction

The study of exotic nuclei is one of the main topics of modern nuclear structure physics. Close to the neutron and proton driplines, respectively, a large variety of formerly unknown nuclear configurations has been observed. Experimentally and also theoretically, efforts are concentrating at present on light exotic nuclei where unexpected phenomena such as neutron [1–3] and proton [4] halos have been observed. For low radioactive beam energies, i.e. for energies near the Coulomb barrier where the transfer cross sections have their maximum, new mass regions extending into medium and heavy nuclei will become accessible in near future by fragmentation and spallation facilities like e.g. SPIRAL [5], EXCYT [6] and REX-ISOLDE [7] or fission fragment facilities as PIAFE [8] or the FRM II at Munich [9]. This will allow to study systematically nuclear matter far off β-stability. The extreme conditions of large charge asymmetry and weak binding provide stringent tests of the concepts of nuclear structure physics which have been obtained from well bound and almost charge symmetric systems.

The purpose of this paper is to explore the use of low energy single nucleon transfer reactions for structure studies of exotic nuclei. As representative examples we consider inverse kinematics reactions with beams of neutron-rich Mg and Sn isotopes. Because of the lack of experimental information on the spectroscopy of such systems results from Hartree-Fock Bogolubov(HFB) calculations for binding energies, wave functions and spectroscopic factors are used. The nuclear structure results are of interest by themselves because nuclear ground states in new mass regions are investigated. The structure input is then used to study single neutron transfer cross sections and angular distributions on several targets, including ^{2}H, ^{9}Be, ^{12}C and ^{24}Mg. The intention is to determine on theoretical grounds suitable conditions and concepts, e.g. with respect to the target nuclei and the incident energy.

In the past, transfer reactions with light and heavy ions have been a major source of spectroscopic information in stable nuclei, including spin and parity assignments to nuclear levels, measurements of occupation probabilities and wave functions in the ground and excited states of the daughter system [10–14]. Provided that beams of exotic nuclei with high enough luminosity will become available it is tempting to use transfer reactions in the same spirit also for spectroscopic studies in exotic nuclei. The important difference to former fixed target experiments is the low intensity of secondary beams and the use of inverse kinematics. Under these conditions only transfer reactions with rather large cross sections can be investigated. Obvi-

ously, the abundance of data to which one is accustomed from work with stable beams can certainly not be expected for radioactive beams. In reactions with inverse kinematics the cross sections are focussed more in forward direction in the laboratory system. Thus, the full yield of the nucleus to be investigated is collected in a rather small angular cone and total cross section measurements should already be feasible at much lower beam intensities. An interesting method to obtain more detailed data on the spectroscopy of bound states is the detection of γ-rays from the decay of excited states in the outgoing system. For stable nuclei the feasibility of such experiments with high resolution was shown e.g. in [15] where a large number of γ transitions could be identified from transfer experiments in inverse kinematics. Since in this case the daughter nucleus is observed directly at an exit energy close to the beam energy, as a clear advantage over the conventional experimental setup, compound processes will be suppressed and clean signals should be observed even on targets as light as a deuteron and for low incident energies.

The central issues of this paper are:

- to explore for which targets and energies the largest cross sections can be expected
- to explore to which extent the reactions are sensitive to nuclear structure and
- to explore the experimental conditions especially for single nucleon pickup reactions in inverse kinematics with low intensity radioactive beams.

In Sect. 2 the description of nuclear structure by Skyrme Hartree-Fock theory is summarized. Results for binding energies, radii and wave functions for $^{20-36}$Mg and $^{100-140}$Sn obtained with the Skyrme interaction of [19] are discussed. The calculations show a number of new and interesting features. In the proton-rich Mg isotopes a rather pronounced proton skin is found which exceeds the neutron distribution by up to 0.3 fm in ^{20}Mg. In the neutron-rich Mg and Sn isotopes the calculations predict rather massive neutron skins. Beyond ^{134}Sn a layer of neutron matter emerges with a thickness of 0.5 fm in the vicinity of ^{140}Sn. Although ^{140}Sn might not be accessible experimentally the onset of this effect should be observable already in $^{132-136}$Sn mass region.

These nuclides are of particular interest because they potentially allow to explore experimentally the full range of isotopes from the proton to the neutron dripline or - in the case of Sn - at least a large part of it. An equally interesting aspect is that in the heavy Mg and Sn isotopes the neutrons start to occupy the (1f,2p)- and the (2f,3p)-shells, respectively. Thus, the neutron-rich Mg and Sn isotopes provide a unique possibility to study nuclear structure far off stability over an energy gap of about 2 oscillator shells for the same spin and parity.

The transfer calculations are performed in the conventional way using DWBA and EFR-DWBA methods for pickup processes on a deuterium and heavier targets, respectively. The theoretical background and numerical methods [10,11] are well established by previous work with stable nuclei. Results on cross sections and angular distributions are discussed in Sect. 3. Empirical optical potentials are taken but separation energies, spectroscopic factors and wave functions from the HF-calculations discussed in Sect.2 are used. An optimum of cross sections is found for incident energies of E_{lab}=2 - 5 MeV/u depending on the projectile-target combinations. In Sect. 3.5 also two-neutron transfer processes are investigated. As an example we discuss the energy dependence of the cross section for the stripping reaction H(^{6}He,^{4}He)t. Such reactions are of special importance for nuclear structure studies of light halo.

In Sect. 4 the implications of the theoretical results on the experimental conditions for transfer reactions with exotic beams with emphasis on the γ-ray spectroscopy are discussed. In Sect. 5 the discussions are summarized and conclusions are drawn.

2 The structure of Mg and Sn isotopes

The nuclear structure calculations have been performed with the Skyrme Hartree-Fock approach [16,17] which is a widely used and successful theory at least for nuclei close to stability. In the past a widespread variety of different Skyrme energy functionals has been derived. They equally well describe stable nuclei but more recent applications to nuclei far off stability are showing considerable deviations when extrapolating into new regions of the mass table [18]. The empirical approach underlying the Skyrme-functionals, however, provides the flexibility to adjust parameters to the new mass regions. In the calculations the interaction of [19] has been used which accounts in a rather satisfactory way for the systematics of β-stable and -unstable nuclei. Parameters were not adjusted for the calculations presented below.

2.1 The Skyrme Hartree-Fock approach

In Skyrme HF-theory binding energies, densities and single particle wave functions are obtained from a local energy functional [16,17]. The parameters are determined empirically, mainly by fits to stable nuclei but also to neutron matter [20]. Microscopically, the Skyrme functional corresponds to an expansion of nuclear interactions up to first order in the momentum transfer [21], i.e. interactions in relative S- and P-waves are included. The nonlocality of the interactions, originating especially from exchange contributions of realistic finite range interactions as a Brueckner G-Matrix [21,22], is described globally by an effective nucleon mass $m^*_q(\mathbf{r})$ which inside a nuclear medium is less than the bare mass m_q in free space. The medium-dependence of nuclear interactions is taken into account effectively by a phenomenological density dependence.

Variation and minimization of the energy functional with respect to the wave functions [17] lead to the single particle Schrödinger equation

$$\left(-\frac{\hbar^2}{2m^*_q(\mathbf{r})}\nabla^2 + W_q(\mathbf{r})\right)\Phi_{qk}(\mathbf{r}) = \varepsilon_{qk}\Phi_{qk}(\mathbf{r}) \quad . \qquad (1)$$

The effective single particle mean-fields - including central and spin-orbit isoscalar and isovector nuclear interactions and for protons also the Coulomb interaction - are denoted by $W_q(\mathbf{r})$ [16,17]. The single particle energies obtained as the eigenvalues of (1) are given by ε_k. A self-consistent solution is sought by recalculating the densities with the wave functions obtained from (1) and iteration of the whole procedure [17].

Pairing for like particles was included in the local density approximation by using the singlet-even interaction obtained from the G-matrix in [22]. The state dependent gap equation was solved [23]. In superconducting systems pairing leads to partial occupation probabilities v_j^2 of the single particle valence levels. The spectroscopic factors $C^2S(\pm)$ for pickup and stripping reactions, respectively, are then defined as (see e.g [13,14])

$$C^2S_j(+) = 1 - v_j^2 \quad , \quad C^2S_j(-) = (2j+1)v_j^2 \qquad (2)$$

and determine the overall magnitude of the cross section aside of kinematical and reaction dynamical contributions.

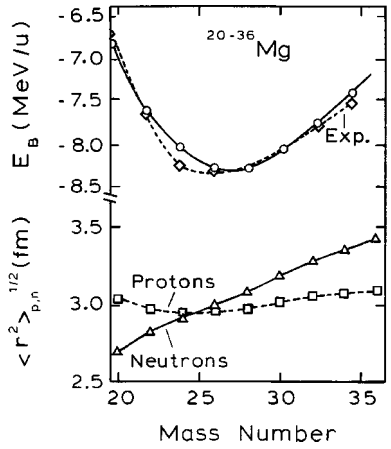

Fig. 1. Binding energies per nucleon (upper part) of Mg isotopes. The theoretical HF-energies (*circles*) are compared to experimental values (*diamonds*) [34]. The binding energy of ^{24}Mg is underestimated because deformation has been neglected (see text). In the lower part, the proton (*squares*) and neutron (*triangles*) rms-radii are shown. Lines are drawn to guide the eye

2.2 Results for Mg isotopes

In the calculations only spherical solutions were considered. This restriction imposes some uncertainties on the Mg results since e.g. ^{24}Mg is known to be deformed [24]. From the comparison of theoretical and experimental binding energies in Fig. 1 it is seen that the energy of ^{24}Mg is indeed underestimated by 0.11 MeV/u (2.8 MeV in the total binding energy) but for the other isotopes the agreement is very satisfactory. From the results it can be concluded that deformation very likely vanishes rapidly aside of ^{24}Mg. The slight overestimation of the ^{32}Mg binding energy might be taken to indicate the recovering of deformation in the heavier isotopes. This would be in agreement with results of a Coulomb excitation experiment [25] where a strong quadrupole transition was observed in ^{32}Mg corresponding to a dynamical deformation parameter β_2=0.5. However, the implications of this result for the possible existence of a statically deformed ^{32}Mg ground state is an open question which deserves further investigations. Theoretically, the proton and neutron driplines are reached at ^{18}Mg and ^{38}Mg, respectively.

The exotic Mg species have been of interest for a long time. After the first production of ^{32}Mg at CERN [26–28] a number of "anomalies" were found with respect to theoretical predictions. In shell model calculations it was realized that the (s,d)-model space is insufficient and a considerable fraction of (1f,2p)-shell occupation must be included [29,30]. These results were confirmed in constrained HF-calculations by Campi et al. [32]. Poves and Retamosa [30] conclude from their shell model calculations that ^{32}Mg is a transitional nucleus. Experimentally, such a behaviour was found already for ^{30}Mg [31]. From the fact that our spherical HF calculations describe the binding energies of the known heavy Mg isotopes rather well it might be concluded that deformation does not contribute significantly to the ground states of these nuclides. However, we do find fractional occupation of the (1f,2p)-shell beyond ^{30}Mg, too.

An interesting phenomenon is observed from the root-mean-square radii (rms) of proton and neutron density distributions displayed in the lower part of Fig. 1. At the proton rich side a proton skin develops which exceeds the neutron density by 0.34 fm in ^{20}Mg. The situation is reversed at the neutron dripline where a neutron skin appears.

Beyond ^{32}Mg the neutrons start to occupy $1f_{7/2}$ orbit and to a less extent, also 2p-states. The valence level approaches rapidly the continuum threshold and in ^{36}Mg a binding energy of only $\varepsilon(1f_{7/2})$=-781 keV is found which leads to the strong increase of the neutron radii in the heavy isotopes. The distribution of the valence neutrons over the (1f,2p)-levels depends in detail much on the pairing interaction. In the present calculation only a small fraction is found in the 2p-levels. However, for asymmetric systems the pairing interaction is not well known and small changes in strength will result in a different scheme. An increase of the 2p-occupation could lead to much larger radii which even might come close to a halo configuration. The reason is that the p-orbits are subject to a much lower centrifugal barrier than the f-waves and thus, at about the same binding energy, would extend to much larger radii.

2.3 Results for Sn isotopes

Binding energies and rms-radii for $^{100-140}$Sn are shown in Fig. 2. The observed energies are reasonably well reproduced but in the average the agreement is not as good as for the Mg case. Calculations with other standard Skyrme parameter sets (Skyrme-3 [16], Skyrme-M [33] interactions) led even to considerable larger deviations. The results indicate problems of these Skyrme interactions, espe-

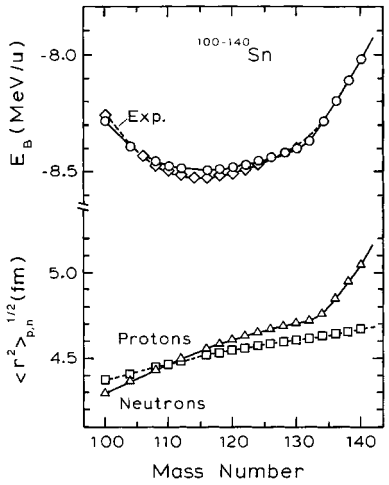

Fig. 2. Binding energies per nucleon (upper part) of the $^{100-140}$Sn isotopes from HF-calculations (*circles*) are compared to data (*diamonds*) [34]). Note the strong decrease of the theoretical binding energies beyond ^{132}Sn which is accompanied by the development of a rather massive neutron skin. In the lower part, the proton (*squares*) and neutron (*triangles*) rms-radii are shown. The rms-radii indicate a proton skin close to ^{100}Sn. The lines are drawn to guide the eye

cially in the isovector channel. The isovector interactions are not well fixed from fits to stable nuclei alone and thus differences may show up depending on the data base used in the determination of the Skyrme parameters. However, the quality of the present Skyrme results is still sufficient for a meaningful comparison to experiment. The neutron dripline is approached around $^{150-152}$Sn where again pairing affects to some extent the exact localization of the dripline. The strong increase of rms-radii beyond ^{130}Sn indicates the formation of a neutron skin in the heavy Sn isotopes. Qualitatively, the same result was found in a recent calculation using a G-matrix interaction [22]. In Fig. 2 it is seen that the onset of this effect is already observable around $^{132-136}$Sn. In this mass region the skin has grown to a thickness of about 0.5 fm which is very sizable by comparison to the value of 0.2 fm found in ^{208}Pb. The short β-decay lifetimes and the strong decrease in production cross sections might inhibit to reach ^{140}Sn but nuclides just below could still be produced. As will be discussed in Sect. 4, transfer reactions could provide a way to overcome the limitations set by the dynamics of production processes.

3 Single neutron transfer reactions on exotic nuclei

3.1 General properties of transfer reactions with exotic nuclei

The new feature in reactions with exotic nuclei is the prevalence of small momentum components in the form factors. Regardless of whether the "prior" or "post" representations [10,11] are chosen the general structure of one-nucleon transfer form factors is such that they are composed of the single particle wave functions Φ of the donor and the acceptor nucleus, respectively, and an interaction potential U describing the dynamics of the transfer process [10,11]. For a reaction leading from an incident channel α=(b+x,B) to the exit channel β=(b,B+x) - populating a weakly bound state in an exotic nucleus $B+x$ - it is instructive to consider the form factor in momentum space. The transfer form factors are then given by folding the Fourier transforms of the wave functions $\Phi_{\alpha,\beta}$ and the interaction $U_{\beta\alpha}$ [35,36]:

$$F(\mathbf{k}_\beta,\mathbf{k}_\alpha) = \int d^3p \Phi^\dagger_\beta(\frac{B}{A}\mathbf{k}_\beta - \mathbf{k}_\alpha - s\mathbf{p}) U_{\beta\alpha}(\mathbf{p}) \times \Phi_\alpha(\mathbf{k}_\beta - \frac{b}{a}\mathbf{k}_\alpha + t\mathbf{p}) \quad , \tag{3}$$

where $\mathbf{k}_{\beta,\alpha}$ are the channel momenta (per projectile nucleon) in the center of mass system and the potential $U_{\beta\alpha}$ absorbs the recoil momentum $\mathbf{p}$. In the post (prior) representation the weight factors become $s=1$ ($s=0$) and $t=0$ ($t=1$). In zero-range approximation, as e.g. used for (d,p) reactions, the expression simplifies to the Fourier transform of the wave function of the state into which the neutron x is transferred and an overall normalization constant [11].

In transfer reactions far off stability the momentum dependence of the form factor and therefore the energy dependence of the cross section is mainly determined by the state Φ_β. The reason is that Φ_β reacts much stronger on small variations of the incident energy (i.e. $\mathbf{k}_\alpha$) and the momentum transfer than the other quantities. For a better understanding it is instructive to consider the limiting case of an unbound state in zero-range approximation. Then, the Fourier transform of Φ_β is given by a δ-function-like distribution centered at the wave number of the continuum state. The Fourier transform of a bound state will peak at momenta of about the inverse of the rms-radius of the populated orbit. Hence, the large rms-radii, typical for valence states in nuclei far off stability, lead to narrower momentum distributions which peak at much smaller momentum than for stable nuclei. Most clearly, this new type of momentum dependence has been seen in high-energy breakup reactions of exotic nuclei, e.g. in [4]. The momentum structure of Φ_β implies for the energy dependence of the cross section a maximum at small incident energies where the position and the width of the energy distribution is determined by the binding energy and the orbital momentum.

On top of these structure effects reaction dynamical contributions are superimposed. For a given target-projectile combination the actual location of the maximum and the magnitude of the cross section are determined by quantities like the height of the Coulomb-barrier, the strength of the absorptive potential, especially for heavier targets, and also the separation energy in the donor nucleus. But once threshold effects are overcome the structure properties are reflected by the dependence of cross sections and angular distributions on incident energy and scattering angle, respectively.

From these considerations it is evident that weakly bound target systems like the deuteron are preferential. Also ^{9}Be with a neutron separation energy of only S_n=1.67 MeV can be expected to be a well suited target. In these cases the reaction is well matched because the Q-value is close to zero. Hence, $|\mathbf{k}_\beta| \simeq |\mathbf{k}_\alpha| \simeq \sqrt{E_{cm}/N}$ and the conditions are such that the cross sections will have a maximum at small incident energies. For well bound targets the Q-value is almost completely determined by the separation energy of the target nucleon and the momentum transfer is at least in the order of the square root of the binding energy per target nucleon. The reaction becomes mismatched over a large range of incident energies and momentum transfers, respectively, resulting in much lower cross sections.

3.2 Neutron pickup on a deuterium target

Single neutron pickup reactions with Mg and Sn isotopes on a deuterium target were calculated in the zero-range DWBA approach including non-locality and finite range corrections [11]. The global optical potential of [38] was used. This potential was also determined for deuteron energies below E_{lab}=20 MeV and has been used in the past as a standard parameter set [38]. From the former experiences with the reaction model and the potential it can be concluded that uncertainties with respect to reaction dynamics should be on a tolerable level. Thus, the results should give a realistic estimate for the yields to be expected experimentally. We also expect that the calculations are reliable enough for meaningful conclusions on nuclear structure effects as contained in the microscopic HF wave functions.

An important question for experiments is which range of incident energies is suited best for transfer reactions on exotic nuclei. In Fig. 3 the angle integrated cross sections for ^{2}H(^{24}Mg,^{25}Mg(5/2^{+}))p, ^{2}H(^{32}Mg,^{33}Mg(7/2^{-}))p and ^{2}H(^{36}Mg,^{37}Mg(7/2^{-}))p are displayed as a function of the incident energy of the Mg isotopes. The ground states of ^{25}Mg(5/2^{+}) and ^{37}Mg(7/2^{-}) are populated while an excited state is reached in the reaction to ^{33}Mg(7/2^{-}). The well bound ^{25}Mg(5/2^{+}) orbit is accompanied by a large reaction Q-value. Therefore, the incident and the exit channels are kinematically strongly mismatched and the cross section never exceeds 2 mb.

The situation changes drastically for ^{33,37}Mg. Here, the Q-values are only of the order of 1 MeV and the good overlap of the scattering wave functions leads to large cross sections. The decrease close to threshold is typical for large orbital angular momentum transfers which here is $L = 3$. The low binding energies of the 7/2^{-} orbital in ^{33,37}Mg is accompanied by a large spatial extension of the wave functions (see Table 1). The small separation energy and large spatial extension of wave functions far off stability lead to an energy-momentum dependence of the cross sections which is very different from those known for transfer reactions on well bound systems.

The cross sections shown in Fig. 3 reach their peak values already at much smaller incident energies than known for (d,p) reactions on stable nuclei. There, one typically finds a maximum around deuteron energies of E_{lab} ≃15-20 MeV [11,12]. For exotic nuclei the calculations predict that the angle integrated cross sections reach an optimum at E_{lab} ≃3-5 MeV/u, much lower than found for stable nuclei. The energy location of the maximum total cross section is almost independent of the projectile-target combination but, as seen below in Sect. 3.3, the magnitude decreases rapidly for well bound heavier (and highly charged) targets.

The differences in width of σ_{tot} for the ^{33,37}Mg(7/2^{-}) energy distributions are caused mainly by the binding energies. The larger extension of the ^{33}Mg(7/2^{-}) wave function leads to an earlier cut off because it is more selective on the momentum transfer window.

Looking to Fig. 4 where angular distributions for the ^{33}Mg reaction are shown reveals that the cross section is shifted to forward directions with increasing incident energy. Over the angular range the momentum transfer

Table 1. Spin and parity, excitation energies, single particle binding energies, spectroscopic factors (see (2)) and root-mean-square radii for states in the Mg and Sn isotopes as obtained from the HF calculations and used in the reaction calculations. For ^{25}Mg the measured neutron separation energy (S_n=7.33 MeV) [34] is used in the transfer calculations

Nucleus	j^π	E_x [MeV]	ε_n [MeV]	$\sqrt{< r^2 >}$ [fm]	$C^2S_j(+)$
^{25}Mg	$\frac{5}{2}^+$	0.0	-6.760	3.36	0.373
^{33}Mg	$\frac{3}{2}^+$	0.0	-4.430	3.87	0.097
^{33}Mg	$\frac{7}{2}^-$	4.019	-0.411	4.51	0.952
^{37}Mg	$\frac{7}{2}^-$	0.0	-0.679	4.58	0.534
^{121}Sn	$\frac{1}{2}^-$	7.404	-0.156	8.01	0.98
^{133}Sn	$\frac{7}{2}^-$	0.0	-2.418	6.16	1.0
^{133}Sn	$\frac{1}{2}^-$	2.33	-0.090	8.17	1.0

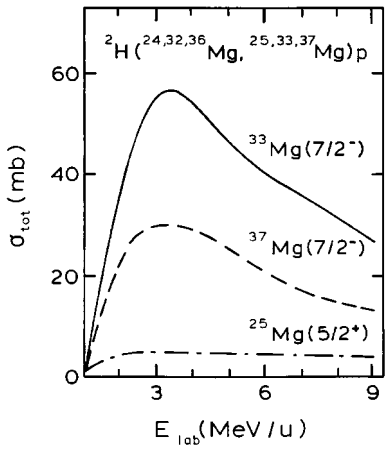

Fig. 3. Dependence of the angle integrated single neutron pickup cross sections on a deuterium target for ^{25}Mg(5/2^{+}, *g.s.*) (*dotted*), ^{37}Mg(7/2^{-},g.s.) (*dashed*) and ^{33}Mg(7/2^{-}) (*full*) on the incident energy per nucleon of the Mg beams

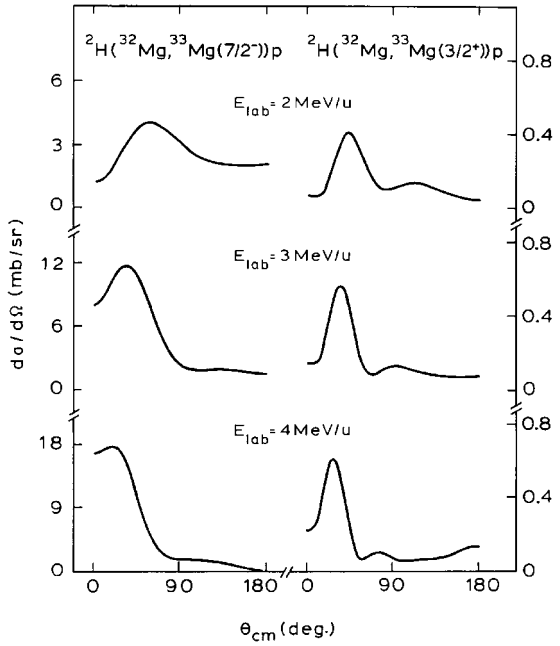

Fig. 4. Angular distributions of single neutron pickup cross sections on a deuteron target for ^{33}Mg(7/2$^-$) (right side) and ^{33}Mg(3/2$^+$,g.s) (left side) at different incident energies of the ^{32}Mg isotope

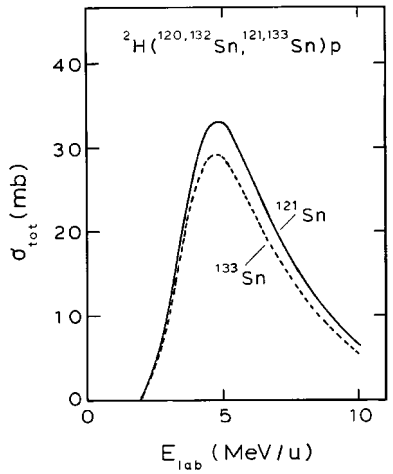

Fig. 5. Dependence of the angle integrated single neutron pickup cross sections on deuterium for ^{120}Sn and ^{132}Sn on the incident energy per nucleon. The lower value of the ^{133}Sn cross section is a combined effect due to the increase of the reaction Q-value (decrease of the binding energy) and quenching of the $3p_{1/2}$ particle strength from pairing

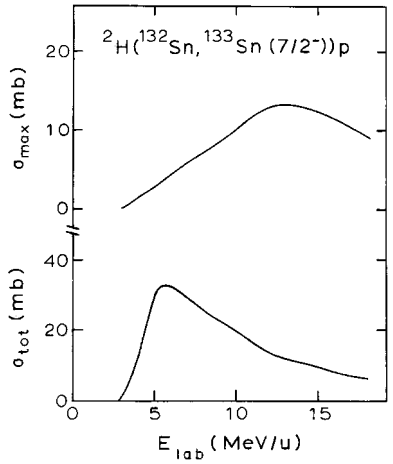

Fig. 6. Dependence of the maximum of the angular distribution (upper part) and the angle integrated (lower part) single neutron pickup cross sections on deuterium leading to ^{133}Sn(7/2$^-$,g.s.) on the incident energy per nucleon

varies from $|k_\alpha - k_\beta|$ to $|k_\alpha + k_\beta|$ such that good momentum matching is obtained only at forward angles. For most of the angular range the reaction becomes mismatched with respect to the momentum and, in particular, the angular momentum transfer. As a result the total cross sections decrease. The same mechanism is responsible also for the fall-off of the ^{37}Mg(7/2$^-$) cross section.

In Fig. 4 also angular distributions for the reaction leading to the ^{33}Mg(3/2$^+$) ground state are shown. The cross sections are much smaller by about a factor of 30 than for the excited state ^{33}Mg(7/2$^-$). The shape is changed because the angular momentum transfer is now $L = 2$. The results illustrate the selectivity of transfer reactions on exotic nuclei to particular configurations. The calculations show that neutron pickup reactions on ^{32}Mg will very likely be dominated by processes leading to weakly bound excited states like ^{33}Mg(7/2$^-$).

Similar observations as for the Mg isotopes hold also for reactions with Sn isotopes. The results might be taken as representative for transfer reactions on heavy exotic nuclides. In Fig. 5 the incident energy dependence of the total cross sections are displayed for the ^{2}H(^{120,132}Sn,^{121,133}Sn(1/2$^-$))p reactions. In both cases the transfers lead to excited $3p_{1/2}$ single particle configurations in the final nuclei. Compared to the ^{33}Mg(7/2$^-$) case the cross sections are smaller by about a factor of 2 but obviously still large enough for measurements and spectroscopic studies, e.g. by γ-ray observation.

In Fig. 6 the energy dependence of the total cross section and the maximum of the angular distribution of the ^{2}H(^{132}Sn,^{133}Sn(7/2$^-$,g.s.))p reaction are shown. The sizable cross section illustrates that low energy transfer reactions indeed might be useful also for investigations of short-lived isotopes in the heavy mass region. Clearly, adding one neutron to ^{132}Sn is an insignificant step in approaching closer to the neutron dripline in that mass region. However, from reactions to the ground states of neighbouring isotopes information is obtained on shell closures and pairing correlations. Both are related to the widely discussed question of shell quenching far off stability. They are complementary to reactions populating excited states which, in the first place, provide access to single particle strength functions and the fragmentation patterns due to particle-core interactions.

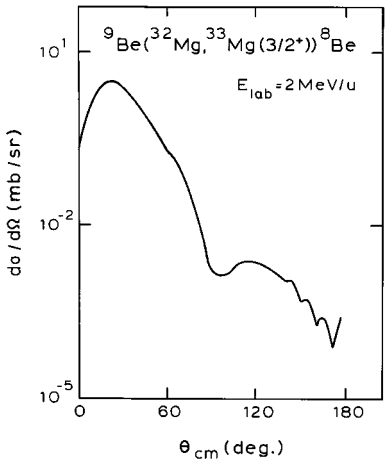

Fig. 7. Angular distribution for the ^{9}Be(^{32}Mg, ^{33}Mg(3/2$^+$,g.s.))^{8}Be reaction at E$_{lab}$=2 MeV/u

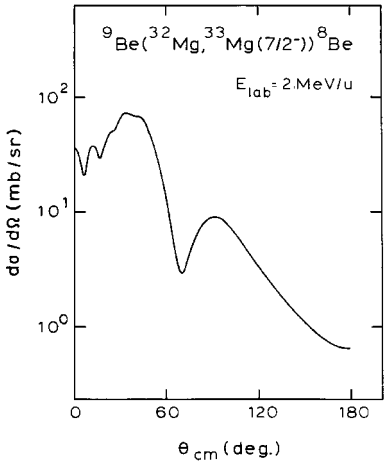

Fig. 8. Angular distribution for the ^{9}Be(^{32}Mg, ^{33}Mg(7/2$^-$))^{8}Be reaction at E$_{lab}$=2 MeV/u

3.3 Single nucleon transfer on heavy targets

In order to account properly for non-locality and recoil effects [11] transfer reaction on targets heavier than the deuteron are described with exact finite range (EFR) DWBA methods [10,13,14,36]. As representative examples pickup reactions with incoming Mg beams on ^{9}Be, ^{12}C and ^{24}Mg targets have been chosen. As a general feature, cross sections decrease rapidly for targets heavier than ^{9}Be. The loss of strength is a combined effect from the increase of the Coulomb barrier and the stronger absorption for larger target charges and masses, respectively. In addition, the reaction Q-values are badly matched for well-bound targets. However, transfer reactions on heavy targets show certain interesting features which allows to obtain valuable complementary information to the deuteron case.

Angular distributions for the reactions ^{9}Be(^{32}Mg,-^{33}Mg(3/2$^+$,g.s.))^{8}Be and ^{9}Be(^{32}Mg,^{33}Mg(7/2$^-$))^{8}Be are displayed in Fig. 7 and Fig. 8, respectively. In magnitude the angle integrated cross sections are even larger than

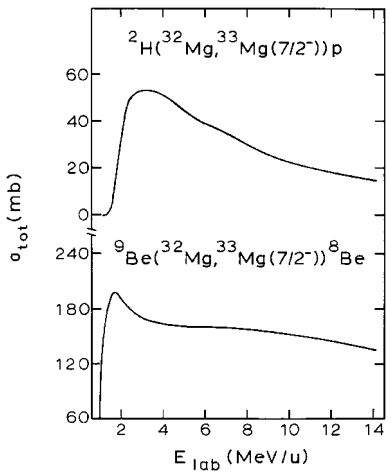

Fig. 9. Dependence on incident energy per nucleon of total transfer cross sections for the (^{32}Mg, ^{33}Mg(7/2$^-$)) reaction on a deuteron (upper part) and a ^{9}Be (lower part) target

for transfer on deuterium. In shape the ^{9}Be angular distributions are much more focussed in forward direction because of stronger absorption and Coulomb repulsion. The reaction mechanism is dominated by nearside scattering. For the transition to the ^{33}Mg ground state (see Fig. 7) a nearside-farside interference is indicated around $\Theta_{cm}\simeq 120°$ and the onset of a rainbow structure becomes visible.

Similar as for the deuterium target the selectivity of the ^{9}Be single nucleon transfer reaction on the asymptotics of the Mg wave function is gradually changing by varying the incident energy. However, decreasing E$_{lab}$ to 1 MeV/u reduces the cross section by about a factor of 3 and the angular distribution is centered around $\Theta_{cm} = 100°$. For higher incident energies the angular distributions become well focussed in forward direction, as indicated already by Fig. 7. Qualitatively the same results have been obtained also for other neutron-rich Mg isotopes and a variety of Na-isotopes.

The energy and Z-dependences of the total cross sections are summarized in Fig. 9 and Fig. 10 where σ_{total} for transfer reactions with ^{32,36}Mg on ^{2}H, ^{9}Be, ^{12}C and ^{24}Mg targets leading to ^{33,37}Mg(7/2$^-$) are shown. The maximum yield is found for the ^{9}Be target. The ^{9}Be cross sections peak at the rather low beam energy of E$_{lab}$ $\simeq$1.8 MeV/u. In case of the deuteron target the maximum yield is located at a slightly higher energy, E$_{lab}$ $\simeq$3 MeV/u with a broader energy distribution. The reactions on ^{12}C lead in the shown energy range to rather small cross sections. At E$_{lab}$ =14 MeV/u values of about 2 mb are found. The cross section for the ^{24}Mg target is somewhat larger because of angular momentum reasons. But even at E$_{lab}$ =14 MeV/u an angle integrated cross section of only about 4 mb is obtained.

Although the magnitude of the cross sections depends in detail on the special conditions of the reaction under consideration the calculations clearly indicate a strong suppression of reactions on highly charged stable nuclei in the low energy region. To a large extent the suppres-

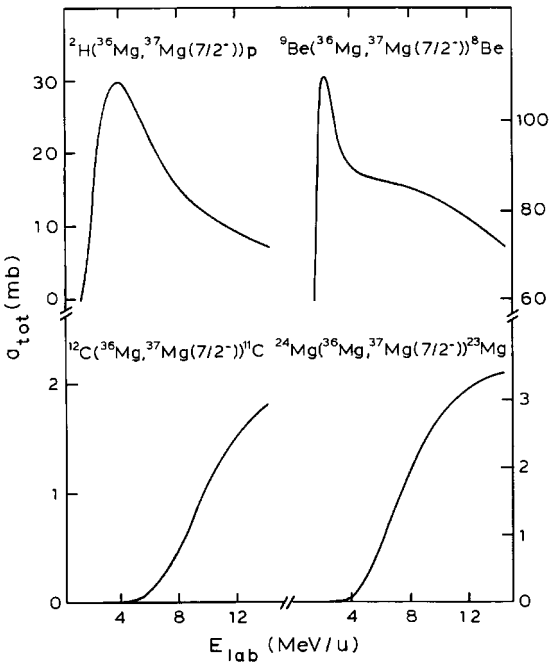

Fig. 10. Dependence on incident energy per nucleon of total transfer cross sections for the (^{36}Mg, ^{37}Mg(7/2$^-$,g.s.)) reaction on a deuteron (upper left), ^{9}Be (upper right), ^{12}C (lower left) and a ^{24}Mg target

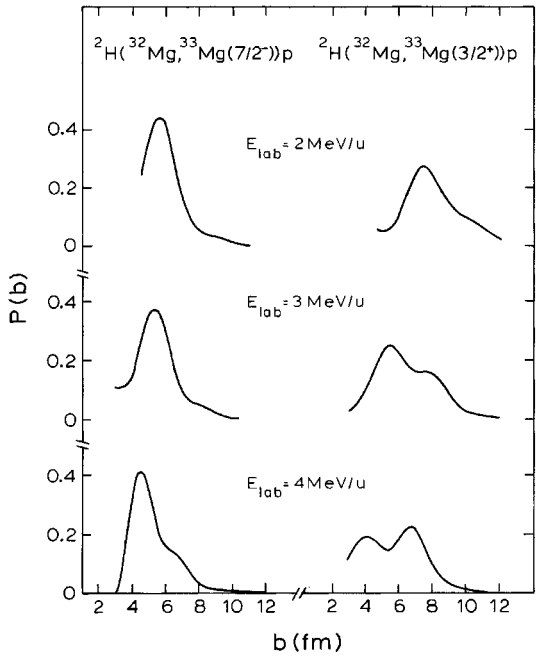

Fig. 11. Impact parameter distribution P(b) of single neutron pickup cross sections on deuterium for ^{33}Mg(7/2$^-$) (left panel) and ^{33}Mg(3/2$^+$,g.s) (right panel) at different incident energies of the Mg isotopes

sion is caused by the comparable high reaction Q-values which typically are Q=-14 to -16 MeV for stable targets. These results recommend to use light targets for reaction studies with exotic nuclei at low incident energies. This observation might be of interest for the design of experimental setups as will be discussed in Sect. 4.

3.4 Impact parameter analysis and spatial location

In Fig. 11, the cross sections for ^{2}H(^{32}Mg,^{33}Mg(3/2$^+$))p and ^{2}H(^{32}Mg,^{33}Mg(7/2$^-$))p are analyzed in terms of impact parameters,

$$b_\ell = \frac{1}{k_\alpha}\left(\eta + \sqrt{\eta^2 + \ell(\ell+1)}\right) \qquad (4)$$

where η is the Sommerfeld Coulomb parameter and k_α the wave number in the incident channel [11]. Since the orbital angular momentum ℓ is quantized a discrete set of b_ℓ-values is obtained initially. A smooth impact parameter distribution P(b) is derived by using

$$P(b) = \frac{1}{\sigma_{tot}} \sum_\ell \int db_\ell \sigma_\ell(b_\ell)\delta(b_\ell - b) \qquad (5)$$

where σ_ℓ denote the quantum-mechanical DWBA partial wave cross sections. Numerically, the Dirac δ-function is replaced by a Lorentzian of finite width $\Gamma_\ell = 0.5(b_{\ell+1} - b_{\ell-1})$ chosen as the average spacing of adjacent (discrete) b_ℓ-values. In the integration a lower cut-off equal to b_0 is used thus excluding the classically forbidden region of impact parameters. The normalization to the angle integrated total cross section σ_{tot} allows to compare results for different reactions in a meaningful way. Although P(b) is not an observable it provides a way to extract theoretically the "classical" aspect of spatial localization from the quantum-mechanical DWBA calculations. Reactions on light targets, as e.g. the deuteron, are dominated by quantum efffects. However, also in such cases it is instructive to consider P(b) in order to obtain a first estimate on the spatial localization of the reaction. P(b) only serves for illustrative purposes and cross sections are being calculated fully quantum mechanically. From Fig. 11 and Fig. 12 it is seen that P(b) depends on the angular momentum transfer, the projectile-target combination and the incident energy. For reactions on deuterium P(b) is well localized at low energies close to the Coulomb barrier. The localization increases with the angular momentum transfer L as indicated by the results for the ^{33}Mg(7/2$^-$) ($L = 3$) and the ^{33}Mg(3/2$^+$,g.s.) ($L = 2$) reactions in Fig. 11. The fall-off towards small impact parameters is a combined effect from the absorptive parts of the optical potential and the Coulomb and centrifugal barriers, respectively. With increasing energy the centroid of the distribution moves gradually to smaller b values. The effect is especially pronounced for ^{33}Mg(7/2$^-$). In the ^{33}Mg(3/2$^+$) case a broad distribution develops at higher energies which reflects the larger mismatch because of the higher Q-value (Q=+2.18 MeV compared to Q=-1.84 MeV for the 7/2$^-$ transition).

A striking feature is observed for the ^{9}Be(^{32,36}Mg, ^{33,37}Mg(7/2$^-$))^{8}Be reactions. Below and around the Coulomb barrier the P(b) distribution is centered far in the

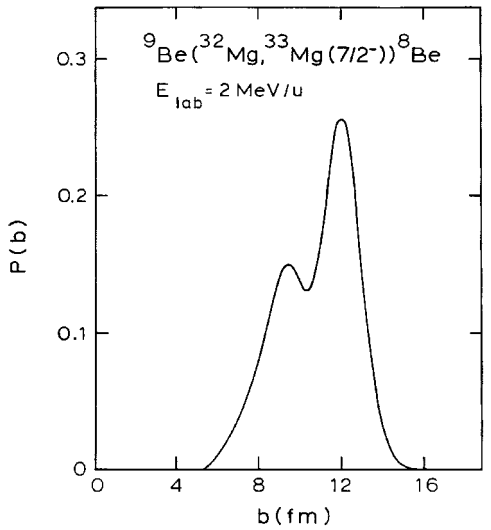

Fig. 12. Impact parameter distribution P(b) at E_{lab}=2 MeV/u for the reaction ^{9}Be(^{32}Mg, ^{33}Mg(7/2$^-$))^{8}Be

asymptotic region with the maximum at b≃12 fm. With increasing energy a second component starts to develop and a gradual shift of strength to smaller impact parameters b≃8.5 fm appears. In Fig. 12 this behaviour is illustrated for ^{33}Mg at E_{lab}=2 MeV/u. At E_{lab} <10 MeV/u both reactions become well localized at the inner b value, corresponding to a distance slightly above the position of the Coulomb barrier (R_C=6.8 fm) for the ^{32,36}Mg+^{9}Be systems.

From these results we conclude that transfer reactions are a suitable tool to probe the tails of wave functions, especially in weakly bound final states. A proper choice of incident energies and projectile-target combinations will allow to scan selectively different regions of the wave functions.

3.5 Two-nucleon transfer reactions

In the previous sections encouraging large cross sections for one neutron transfer reactions with exotic nuclei were obtained. The question arises whether two– and multi–nucleon transfer reactions could lead to an equally favorable situation.

As discussed by Bohlen et al. [37] cross sections decrease very rapidly with the number x of transferred nucleons ("xN" processes). With respect to the reaction yields it is in most cases preferable to produce an isotope A with an A-1 radioactive beam and a subsequent single nucleon transfer reaction than by xN multi-nucleon transfer reactions from a beam of stable nuclei [37]. An important reason is that the dynamics of xN-processes are not in favor of transferring a multi-nucleon cluster of a single kind of particles. The driving forces are directed towards charge-equilibration and, as a consequence, the transfer of a mixture of protons and neutrons is dynamically preferred. Also the xN-Q-values are much larger and in order to obtain measurable cross sections incident energies well above 10 MeV/u are required.

Two–neutron transfer reactions play a special role in studying light halo nuclei as ^{6}He and ^{11}Li. For such investigations stripping reactions in which the valence cluster is stripped off are of particular interest. Here, we consider only low energy two neutron stripping reactions with inverse kinematics. They will in principle provide nuclear structure information complementary to the one obtained from breakup reactions or even allow a more direct access to the dynamics of halo nucleons. In order to obtain a well–matched reaction an appropriate choice of targets providing a low reaction Q–value is of particular importance. For the choice of the target, advantage can be taken of the fact that the stripping process leads to neutron–rich target daughter nuclei. Hence, the reaction Q–value is controlled by the two–neutron separation energies in the final target–like residue rather than by the binding properties of the initial stable target as in pickup reactions. For stripping reactions with inverse kinematics this allows to use processes leading to unstable isotopes of the initial target nucleus.

Favorable cases are e.g. two–neutron stripping reactions on a hydrogen or a deuterium target in which the target residue is a triton (S_{2n}(t)=8.481 MeV) or a ^{4}H nucleus (S_{2n}(^{4}H)=3.351 MeV) [34]. But also (^{4}He,^{6}He), (^{7}Li,^{9}Li) and (^{9}Be,^{11}Be) reactions with S_{2n}(^{6}He)=0.973 MeV, S_{2n}(^{9}Li)=6.096 MeV and S_{2n}(^{11}Be)=7.316 MeV, respectively, are suitable. For heavier stable nuclei the two–neutron (and also two–proton) separation energies in the daughter nuclei are ranging typically around $S_{2n} \simeq$ 20 MeV - 30 MeV [34]. In reactions involving well bound stable nuclei in both the incident and the exit channels the large separations energies are likely to cancel and in total a moderate Q–value is found. Obviously, such a cancellation does not occur when a weakly bound exotic nucleus is participating in the reaction. Such reactions are likely to become energetically mismatched and low cross sections have to be expected. Hence, a situation is encountered similar to the single neutron transfer reactions discussed previously. There, the largest cross sections were also obtained for targets with small single particle binding energies.

At low energies the reaction mechanism of two–nucleon transfer reactions, however, is of a more complicated nature. Two–step processes, involving the sequential transfer of two single nucleons, and one–step cluster transfer reactions contribute coherently to the cross sections. The sequential processes reveal interesting details of the reaction mechanism of exotic nuclei but clearly they inhibit the direct access to nuclear structure information. For that purpose the cluster transfer process provides a clearer signature on the spectroscopy and wave functions of e.g. two neutron halo configurations.

These features are illustrated for the H(^{6}He,^{4}He)t reaction in Fig. 13. The total cross section is shown as a function of the incident energy of ^{6}He. In the calculations the sequential two–step transfer of the neutrons through the ^{5}He(3/2$^-$,1.87 MeV) resonance as an intermediate state

and the one–step cluster transfer of a two–neutron cluster are taken into account. For the cluster transfer the two neutrons were assumed to be in a relative s-wave state. The motion of the cluster with respect to the core was described by a 2s wave function. The maximum around E_{lab}=2.5 MeV is caused by the two–step processes. Close to the threshold they are suppressed because they involve twice an L=1 transfer. Since the direct process proceeds through L=0 transfer the cross sections retains a finite value close to the reaction threshold reflecting the two–neutron scattering length on the target. In magnitude, the cross sections are considerably reduced compared to the single nucleon pickup reactions.

From Fig. 13 it is seen that for a (^{6}He,^{4}He) reaction the direct and sequential contributions interfere destructively at low energies. The sequential contributions are found to decrease steadily beyond $E_{lab} \simeq$14 MeV/u. The calculations predict that direct cluster transfer prevails only at energies around or above 20 MeV. Hence, for a direct observation of cluster properties incident energies of at least 20 MeV should be chosen. At low energies, however, two–neutron stripping reactions give access to the reaction dynamics of exotic nuclei.

The increase of the two–step contributions at low energies reflects again the fact that the form factors include weakly and even unbound single particle states. Thus, in each step a situation is encountered which is similar to the dynamics of the single neutron one–step transfer reactions discussed in the earlier sections.

Former attempts to describe two–nucleon transfer reactions indicate that the reaction dynamics and possibly also the nuclear structure aspects of these processes are less well understood than for single nucleon transfer reactions. Typically, calculations have a tendency to underestimate the measured cross sections. Also, the results are sometimes found to depend sensitively on the optical potentials. Simultanuous measurements of elastic scattering in the initial and the final channels together with the transfer cross section could reduce the uncertainties related to optical potentials. Despite these uncertainties, the results of Fig. 13 can be expected to describe at least qualitatively the typical features of two–neutron transfer processes of halo nuclei.

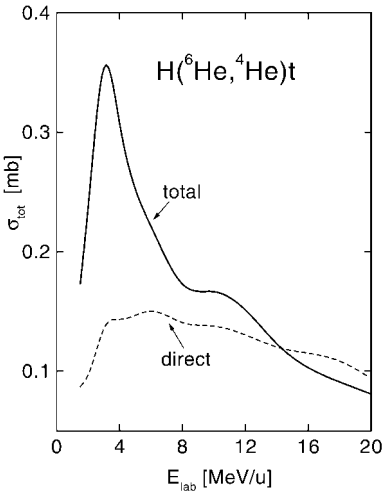

Fig. 13. Dependence of the total cross section H(^{6}He,^{4}He)t on the incident energy. Contributions from sequential two–step transfer processes through the ^{5}He($3/2^-$,1.87 MeV) resonance and the direct transfer of a two neutron cluster are included coherently into the total cross sections. The direct partial cross sections are shown also separately

4 Experimental aspects of transfer reactions with exotic beams

Experimentally, single and few nucleon transfer reactions were studied extensively in the past with stable beams, e.g. [13–15]. For exotic beams, however, as mentioned before, two main experimental differences are present: the use of inverse kinematics and the low beam intensities. In addition, also the importance of minimizing beam induced background events from the decay of β-instable nuclei and daughter activities requires special attention.

Since exotic beams are obtained as secondary beams they depend on the production rates for unstable nuclei in primary reactions with stable beam. As a consequence, their intensities are reduced by several orders of magnitude with respect to the intensities of the primary beam. As a rough rule, the production cross sections for these beams fall by approximately one order of magnitude for each mass unit going further away from stability, regardless of the production mechanism. Thus, one is restricted to reactions with rather large cross sections. Targets should be chosen as thick as possible and detectors with large solid angles and high detection efficiency should be used.

In principle a large variety of single and few nucleon transfer reactions may be investigated experimentally. However, as it was shown in previous sections, mainly the cross sections for single neutron transfer reactions on deuterium and ^{9}Be targets at low incident energies are large enough (in the order of a few times of ten millibarns to about 100 mb) to perform experiments with the low secondary beam intensities. As it was shown in Sect. 3.3 the decrease of cross section to heavier masses is the result of a combined effect in the increase of the Coulomb barrier, the stronger absorption and the badly matched reaction Q-value for well bound targets. The latter fact may be overcome by using in case of single neutron transfer reactions neutron rich target isotopes like e.g. ^{13}C or ^{14}C. However, such targets are expensive and difficult to obtain.

Single nucleon transfer reactions are binary reactions and the reaction mechanism is well enough established from the previous investigations on stable nuclei. Transfer reactions have several features which make them very attractive for experimental work. For applications to exotic nuclei it is worthwhile to emphasize that

– the maximum transfer cross section are relatively large. As it has been shown in the previous sections cross sections of a few 10 mb to about 100 mb can be expected.

– they are selective on the single particle properties of exotic nuclei while other non-elastic processes like Coulomb excitation reactions mainly probe the collective properties of nuclei,
– for pick-up reactions with beam particles of mass A the (A+1)- and (Z+1)-isotopes can be measured in neutron and proton transfer processes, respectively. Hence, an additional step away from stability by one mass unit is done.
– the single nucleon transfer cross section are largest for ^{2}H - for neutron transfer also for ^{9}Be - targets and drop off very rapidly with targets of higher Z.

For a cross section of 10 mb with a luminosity of 10^{26} $cm^{-2}s^{-1}$ a reaction rate of 1 s^{-1} is achieved. With a fully deuterated polyethylene target of 1 mg/cm^2 which contains $0.75*10^{21}$ deuterium atoms these luminosities are obtained with beam intensities of in the order of 10^5 particles/s. The raise of the calculated cross sections for weakly bound nuclei shows that the dynamics of transfer reactions is favorable for systems far off stability and experiments can very likely take advantage of this behaviour. The rapid decrease of cross section with the target charge has the experimental advantage that in case of deuterated polyethylene target compounds or deuterium gettered Ti targets counts from reactions on the backing material are negligibly small [15] and spectra almost free of target background reactions can be expected.

In order to study single nucleon transfer reactions to resolved final states mainly three experimental techniques exist:

1. Detection of the light target-like nucleus. For reactions on light targets in inverse kinematics the energy of the reaction products strongly depends on their angle in the laboratory system. To resolve states in the final nucleus rather good energy and angle resolution must be achieved. Targets must be rather thin to avoid large energy losses and angular straggling, good beam qualities as well as a high detector granularity are required. Experimental conditions for the detection of the light target-like charged particle are discussed in more detail in reference [39] where also concepts in using active targets are given.
2. Detection of the heavy projectile-like nucleus. The direct observation of the heavy reaction products has the advantage that compound processes are suppressed which in the previous case will spoil the measurements, especially at low incident energies and for low-Z targets. Since in inverse reactions with low mass targets the recoil direction of the heavy reaction product is well defined in the laboratory system (beam direction) it may be identified with the help of a magnet in conjunction with time-of-flight and/or ΔE methods in a small forward angular cone with nearly the efficiency of a full 4π measurement. For the detection of the projectile-like nucleus with suitable experimental resolutions thin targets have to be used. However, since in this case beam and reaction products have the same or nearly the same Z and the velocities do not differ much the energy loss does not depend on the position of the reaction in the target and is constant. Thus, experimental resolutions are affected only by energy and angular straggling. At least the detection of the heavy recoil nucleus may be used as a reaction trigger and to determine the total cross section.
3. Detection of γ-rays to measure the de-excitation of excited bound states in the heavy projectile-like nucleus. High resolution γ-ray detection in single nucleon transfer reactions in inverse kinematics is a promising method. Because it is most effective for very light targets as ^{2}H and ^{9}Be it has several advantages over the previous cases. This was demonstrated experimentally e.g. in [15] where neutron and proton transfer reactions with Ar beams on a deuteron target were investigated at E_{lab}=1.4 MeV/u. A possible concept for such experiments in combination with charged particle detection is shown schematically in Fig. 14.

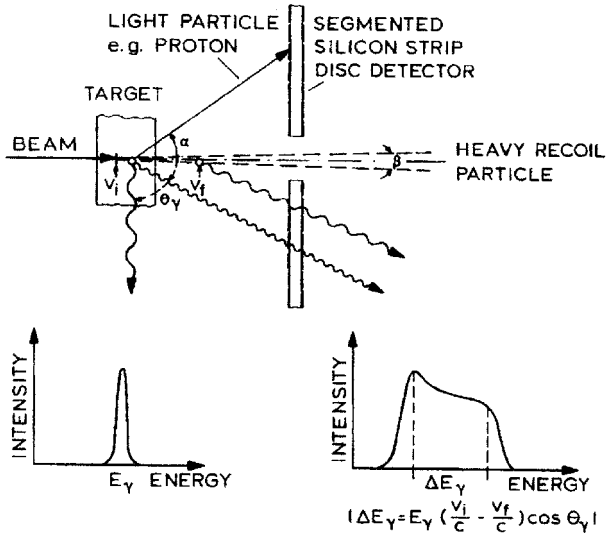

Fig. 14. A schematic outline of an experimental set-up to measure e.g. the inverse reactions on a deuterium target is shown in the upper part of the figure. The proton can be measured in a segmented silicon strip detector, the heavy recoil by means of a magnet in conjunction with time-of-flight and/or ΔE methods while the γ-rays may be detected in a compact Ge-array [41, 42]. In the lower part two γ-spectra are sketched. Left side at 90^0 with respect to the beam and non Doppler-shifted. Right side an γ line shape obtained by Doppler-shift attenuation

As mentioned above the recoil direction of the heavy particle in inverse reactions is well defined in the laboratory system (beam direction). The γ-detection and γ-emission angles, respectively, are equal. A trigger on an emitted particle angle is not compellingly needed which allows to use thick targets. Thus, spectroscopy of exotic nuclei with resolutions in the keV-region can be performed with rather thick targets. Recent Coulomb excitation measurements in ^{32}Mg indicates a large deformation [25] of $\beta_2 \approx 0.5$. In such cases single particle states will be strongly fragmented by coupling to rotational core excitations and the observation of the fragmentation pattern in

transfer reactions will require an excellent energy resolution.

If the beam is not stopped in the target material but dumped in a shielded cup or moved e.g. by a rotating target disc or belt to a shielded area the background contributions from the β and γ decays of beam particles can be minimized. According to the strong fall-off of transfer cross sections on heavier target nuclei the background originating from reactions on the target compounds will be negligible. For example, in single neutron transfer reactions on a deuterated polyethylene target at energies where the cross section has its maximum, the transfer cross section on carbon is lower by more than two orders of magnitude as shown in Fig. 10. However, an important background source may come from single and multiple Coulomb scattering of beam particles to larger angles where they are deposited in the detectors and the walls of the scattering chamber.

Besides a precise measurement of excitation energies also lifetimes of excited states can be determined from high resolution γ-energy spectra. In an inverse reaction the velocity of the projectile-like product is practically equal to the beam velocity, e.g. for beam energies ranging from 2-5 MeV/u the recoil velocities are ranging from 6% to 10% of the velocity of light. Doppler-shifts much larger than the energy resolution of the γ-detectors are thus achieved and the lifetimes can be measured by Doppler-shift attenuation or plunger methods rather precisely [15, 40]. In case of the plunger method, for example, this is achieved by measuring the intensity ratio of the fully Doppler-shifted (decay after the target foil) to the less shifted energy of the γ-rays after the transmission through a plunger foil. The majority of nuclear levels decaying by γ-rays have lifetimes of the order of 10^{-14} s to 10^{-9} s and this time region is covered almost completely by these two methods. In order to avoid large background counting rates in Doppler-shift measurements it is again important not to stop the radioactive beam completely.

In single nucleon transfer reactions where mostly low-lying levels with low spin are populated typical γ-energies and multiplicities are low. The energy resolution is mainly limited by Doppler-broadening resulting from the opening angle of the γ-detectors which, in turn, is anyway limited by the opening angles of the recoiling nuclei. Thus, a compact Ge-detector array may be used, e.g. the Miniball [41].

Typical efficiencies for the detection of the full energy such Ge-detectors are $\epsilon \approx 30\%$ and 4π detection efficiencies of 20% can be achieved. From the angular distributions in Fig. 4 it is seen that a large part of the cross section is concentrated in a small range of center-of-mass angles. In the laboratory system the angular range is even smaller. These are favorable conditions which may allow to measure particle-γ correlations even for beams of low intensity. Since in transfer reactions a spin alignment is produced in the final states of the outgoing nuclei [11] and since the differential cross section is concentrated at a certain angle spins of excited states in the outgoing nuclei may already be deduced from measuring γ-angular distributions.

5 Summary and conclusions

Ground-state properties as binding energies and root-mean-square radii of $^{18-36}$Mg and $^{100-140}$Sn isotopes were obtained from HF calculations using a standard Skyrme interaction [19]. Because the experimentally known binding energies were described reasonably well an extrapolation into regions far off β-stability is meaningful. Both for Mg and Sn extended neutron and proton skins were found close to the driplines. The theoretical single particle energies, occupation probabilities and wave functions were used to explore single neutron transfer reactions with exotic nuclei. Since β-unstable nuclei are produced as secondary beams reactions with inverse kinematics must be used. Since single nucleon transfer reactions are binary processes the interpretation of the results is comparatively simple and decisive answers on nuclear structure and also insight into the reaction dynamics of exotic nuclei can be expected. Transfer reactions on a deuterium target were described in zero-range DWBA. For heavier targets EFR-DWBA methods have been applied which account properly for recoil effects.

As representative examples single neutron transfer reactions with neutron-rich Mg and Sn isotopes were considered. The calculations predict that transfer reactions on deuterium and ^{9}Be targets are most favorable for experiments. The large cross sections, ranging from a few of tens of millibarns to about 100 mb, will allow to use these reactions even with beams of low intensity. The strong decrease of transfer cross sections with target mass at low energies is a clear advantage for experimental work because background from transfer reactions on high-Z target material will be strongly reduced.

Different to the experience with stable nuclei the cross sections reach their maximum at rather small incident energies. This behaviour was shown to be directly related to the special properties of wave functions in weakly bound exotic nuclei. In particular, the mechanism also favors transfer reactions into excited states of the daughter nucleus. This provides access to the spectroscopy of exotic nuclei. From an impact parameter analysis the transfer reactions were found to proceed well beyond the nuclear surface showing that the tails of the wave functions are predominantly tested. For two-neutron transfer reactions important contributions of sequential single nucleon processes were found to determine the cross sections at low incident energies.

Experimental aspects and conditions were discussed. For reactions populating the ground state of the daughter nucleus the detection of the outgoing heavy fragment is an appropriate method because contributions from compound reactions are absent. For spectroscopic work a promising experimental approach is to measure the γ-rays emitted in the de-excitation process of reactions products.

Despite the uncertainties on optical potentials which, in fact, are important for a precise description of transfer cross sections, the results can be expected to describe realistically the dynamical features of such reactions. A clear improvement for future work and the analysis of data would be achieved by measuring elastic scattering together

with transfer reactions such that empirical information on optical potentials is obtained.

This work is supported in part by DFG (Contract Le 439/1), GSI Darmstadt and the German Ministry of Education and Research (BMBF), under contract 06DA820. Enlightening discussions with H.G. Bohlen, HMI Berlin, and G. Walter, IReS Strasbourg, are gratefully acknowledged.

References

1. I. Tanihata, J. Phys. **G** : Nucl. Part. Phys. **22** 157 (1996)
2. P.G. Hansen, A.S. Jensen and B. Jonson, Ann. Rev. Nucl. Part. Sci. **45** 591 (1995)
3. L.N. Ostrowski, H.G. Bohlen, A.S. Demyanova, B. Gebauer, R.Kalpakchieva, Ch. Langner, H. Lenske, M. von Lucke-Petsch, W. von Oertzen, A.A. Oglobin, Y.E. Penionzhkevich, M. Wilpert and Th. Wilpert, Z. Phys. **A343** 489 (1992); H.G. Bohlen, B. Gebauer, M. von Lucke-Petsch, W. von Oertzen, A.N. Ostrowski, M. Wilpert, Th. Wilpert, H. Lenske, D.V. Alexandrov, A.S. Demyanova, E. Nikolskii, A.A. Korsheninnikov, A.A. Oglobin, R.Kalpakchieva, Y.E. Penionzhkevich and S. Piskor, Z. Phys. **A344** 381 (1993)
4. W. Schwab, H. Geissel, H. Lenske, K.H. Behr, A. Brünle, K. Burkard, H. Irnich, T. Kobayashi, G. Kraus, A. Magel, G. Münzenberg, F. Nickel, K. Riisager, C. Scheidenberger, B.M. Sherrill, T. Suzuki and B. Voss, Z. Phys. **A350** 283 (1995)
5. Proposal for the SPIRAL project, GANIL internal report 1995
6. G. Ciavola, L. Calabretta, G. Cuttone, G. Di Bartolo, P. Finocchiaro, S. Gammino, M. Gu, E. Migneco, J. Qin, G. Raia, D. Rifuggiato, A. Rovelli, D. Vinciguerra and H. Wollnik, Proc. of the Fourth Int. Conf. on Radioactive Nuclear Beams, Omiya, Japan, Nucl. Phys. **A616** 69c (1997)
7. D. Habs, O. Kester, G. Bollen, L. Liljeby, K.G. Rensfelt, D. Schwalm, R. von Hahn, G. Walter, P. van Duppen and the REX-Isolde collaboration, Proc. of the Fourth Int. Conf. on Radioactive Nuclear Beams, Omiya, Japan, Nucl. Phys. **A616** 29c (1997)
8. Overview of the PIAF project, Internal Report, ISN Grenoble, June 1994
9. D. Habs, O. Kester, P. Thirolf, K.E.G. Löbner, H.J. Maier, D. Rudolph, U. Schramm, T. Faestermann, G. Hinderer, P. Kienle, U. Köster, H.-J. Körner, E. Steichele, A. Ulrich, T. von Egidy, H. Faust and M. Groß, Proc. of the Fourth Int. Conf. on Radioactive Nuclear Beams, Omiya, Japan, Nucl. Phys. **A616** 39c (1997)
10. T. Tamura, Phys.Rep. **14** 59 (1974)
11. G.R. Satchler, Direct Nuclear Reactions, Oxford University Press, Oxford, 1982
12. F.J. Eckle, H. Lenske, G. Eckle, G. Graw, R. Hertenberger, H. Kader, F. Merz, H. Nann, P. Schiemenz and H.H. Wolter, Phys. Rev. **C39** 1662 (1989); F.J. Eckle, H. Lenske, G. Eckle, G. Graw, R. Hertenberger, H. Kader, H.J. Maier, F. Merz, H. Nann, P. Schiemenz and H.H. Wolter, Nucl. Phys. **A506** 159 (1990)
13. C. Brendel, P. Von Neumann-Cosel, A. Richter, G. Schrieder, H. Lenske, H.H. Wolter, J. Carter and D. Schüll, Nucl. Phys. **A477** 162 (1988)
14. P. von Neumann-Cosel, A. Richter, H.-J. Schmidt-Brücken, G. Schrieder, H. Lenske, H.H. Wolter, J. Carter, R. Jahn, B. Kohlmeyer and D. Schüll, Nucl. Phys. **A516** 385 (1990)
15. G. Schrieder, A. Müller-Arnke and A. Richter, Nucl. Phys. **A279** 463 (1977)
16. D. Vautherin and D.M. Brink, Phys. Rev. **C5** 626 (1972)
17. P. Ring and P. Schuck, The Nuclear Many-Body Problem, Springer, Berlin 1980
18. P.G. Reinhard, private communication
19. J. Friedrich and P.G. Reinhard, Phys. Rev. **C33** 335 (1986)
20. E. Chabanat, P. Bonche, P. Haensel, J. Meyer and R. Schaeffer, preprint Univ. Lyon, Nov. 1996
21. J.W. Negele and D. Vautherin, Phys. Rev. **C1** 1472 (1972)
22. F. Hofmann and H. Lenske, Phys. Rev. **C**, in print, see nucl-th/9705049
23. J. Decharge and D. Gogny, Phys. Rev. **C21** 1568 (1972)
24. A.E. Litherland, H. McManus, E.B. Paul, D.A. Bromley and H.E. Grove, Can. J. Phys. **36** 378 (1958)
25. T. Motobayashi, Y. Ikeda, Y. Ando, K. Ieki, M. Inoue, N. Iwasa, T. Kikuchi, M. Kurokawa, S. Moriya, S. Ogawa, H. Murakami, S. Shimoura, Y. Yanagisawa, T. Nakamura, Y. Watanabe, M. Ishihara, T. Teranishi, H. Okuno and R.F. Casten, Phys. Lett. **B346** 9 (1995)
26. C. Thibault, R. Klapisch, C. Rigaud, A.M. Poskanzer, R. Prieels, L. Lessard, W. Reisdorf, Phys. Rev. **C12** 644 (1975)
27. C. Detraz, M. Langevin, M.C. Goffri-Kouassi, D. Guillemaud, M. Epherre, G. Audi, C. Thibault and F. Touchard Nucl. Phys **A394** 378 (1983)
28. D. Guillemaud-Mueller, C. Detraz, M. Langevin, F. Naulin, M. de Saint-Simon, C. Thibault and F. Touchard, Nucl. Phys. **A426** 37 (1984)
29. W. Chung and B.H. Wildenthal, Phys. Rev. **C22** 2260 (1980)
30. A. Poves and J. Retamosa, Phys. Lett. **184** 311 (1987)
31. G. Klotz, P. Baumann, M. Bounajma, A. Huck, A. Knipper, G. Walter, G. Marguier, C. Richard-Serre, A. Poves and J. Retamosa, Phys. Rev. **C47** 2502 (1993)
32. X. Campi, H. Flocard, A.K. Kerman and S. Koonin, Nucl. Phys. **A251** 193 (1975)
33. H. Krivine, J. Treiner and O. Bohigas, Nucl. Phys. **A336** 155 (1980)
34. G. Audi and A.H. Wapstra, Nucl. Phys. **A595** 409 (1995)
35. W. von Oertzen, Phys. Lett. **151B** 95 (1985)
36. H. Lenske, H.G. Bohlen and H. Wolter, Phys. Rev.Lett. **62** 1457 (1989)
37. H.G. Bohlen, W. von Oertzen, Th. Stolla, R. Kalpakchieva, B. Gebauer, M. Wilpert, Th. Wilpert, A.N. Ostrowski, S.M. Grimes and T.N. Massey, Nucl. Phys. **A616** 254c (1997)
38. W.W. Daehnick, J.D. Childs and Z. Vrcelj, Phys. Rev. **C21** 2253 (1980)
39. P. Egelhof, Proceedings of the Int. Workshop on Research of Fission Fragments, Benediktbeuern 1996, ed. T. v. Egidy, World Scientific 1997, p. 178
40. D.Schwalm and D.Pelte, in Heavy Ion Collisions Vol.**3**, ed. by R.Bock, North-Holland Publishing Company, 1982, p.1
41. D. Habs, D. Rudolph, P.Thirolf, C. Fischbeck, Ch. Gund, D. Schwalm, J. Eberth, E. Grosse, H. Prade, H. Emling, J. Gerl, R.M. Lieder, P. van Duppen, C. Rossi-Alvarez and M. Pionanelli, Progress in Particle and Nuclear Physics, Vol. **38** 111 (1996)
42. A. Huck, REX-ISOLDE meeting, CERN, Oct. 1996